Fusion of a neutron skin nucleus: The ^{209}Bi(^{6}He,4n) reaction

P. A. DeYoung, B. Hughey, P. L. Jolivette, and G. F. Peaslee
Department of Physics, Hope College, Holland, Michigan 49422-9000

J. J. Kolata, V. Guimarães, D. Peterson, and P. Santi
Physics Department, University of Notre Dame, Notre Dame, Indiana 46556

H. C. Griffin and J. A. Zimmerman
Chemistry Department, University of Michigan, Ann Arbor, Michigan 48109

J. D. Hinnefeld
Physics Department, Indiana University–South Bend, South Bend, Indiana 46615
(Received 6 July 1998)

This report details a greatly improved measurement of the four-neutron evaporation cross section following the fusion of ^{6}He$+^{209}$Bi for center-of-mass energies between 23.5 and 30.7 MeV. The results, for energies above the Coulomb barrier, are interpreted within the context of the standard statistical model.
[S0556-2813(98)01312-0]

PACS number(s): 25.70.Jj

I. INTRODUCTION

The development of radioactive nuclear beams at several laboratories allows the study of nuclei with novel and interesting properties. Of particular interest are nuclei such as ^{11}Li (which, because the valence neutrons are found well outside the core ^{9}Li, is considered a neutron-halo nucleus) and ^{6}He (which has valence neutrons somewhat outside a ^{4}He core and so is considered a neutron-skin nucleus). Such nuclei are remarkable because of their extended size, their level structure (which may include low-lying $E1$ states [1]), and because they become unbound if any part of the system is removed (''Borromean nuclei'' [2]). Such features should influence the interactions of these exotic species with other nuclei.

Many theoretical predictions have been made for the fusion of ^{11}Li near the Coloumb barrier [3–7]. However, there is no consensus about the effects of the various exotic properties on the fusion probability and subsequent decay. Many calculations include a lower barrier due to the larger-than-normal radius and coupling to the soft $E1$ mode which works to enhance the fusion cross section [3]. Other groups have included the role of projectile breakup and have concluded that there may be a reduction of the fusion yield and that the excitation function may have structure near the Coulomb barrier [4–6]. This prediction is not universally accepted [7].

The effects on the reaction mechanisms due to the exotic structure of these nuclei are expected to be greatest in ^{11}Li because of its halo nature. However, the effects predicted for ^{11}Li are also expected for ^{6}He. (Currently, ^{6}He beams of the appropriate energy are more intense and of higher quality than ^{11}Li.) In the case of ^{6}He there is a neutron skin outside an α particle core even though the wave function is not as extended as in the case of ^{11}Li [8].

In this paper we report on the cross section for the evaporation of four neutrons emitted following the fusion of ^{6}He $+^{209}$Bi for beam energies between 24.1 and 31.6 MeV. The four-neutron evaporation cross section was measured by first irradiating Bi targets and then counting the delayed α-activity off-line. There was one previous measurement of the four-neutron cross section by the Flerov Laboratory for Nuclear Reactions in Dubna, Russia [12]. However, this measurement had poor energy resolution and large error bars. The cross section for fission following fusion for this system was also measured by a group at Dubna [12,13], as well as at the Nuclear Structure Laboratory at the University of Notre Dame [14].

II. EXPERIMENTAL PROCEDURE AND DATA ANALYSIS

The present measurement is based on the particular decay properties of ^{211}At, which is the residual nucleus following four-neutron evaporation from the ^{215}At compound nucleus. The ^{211}At nucleus has a 7.2 h half-life. When it decays, it emits a 5.87 MeV α particle (41.8%) or decays by electron capture (58.2%) to ^{211}Po (half-life of 0.52 s) which emits a 7.45 MeV α particle. This long parent half-life makes it possible to irradiate Bi targets, build up a significant amount of ^{211}At in the targets, and then determine the production cross section by counting the α decay rate off-line.

A radioactive ^{6}He beam was produced at the Nuclear Structure Laboratory of the University of Notre Dame. A large superconducting solenoid magnet (the *TwinSol* system) collected and focused the secondary ^{6}He produced by the ^{7}Li$+^{9}$Be reaction onto the ^{209}Bi targets. (Additional details of the *TwinSol* installation at Notre Dame can be found in Refs. [9–11].)

The secondary ^{6}He beam of 32.5 MeV passed though a Au target (for beam monitoring purposes) and then through an alternating sequence of targets and energy degrading foils to simultaneously irradiate 16 ^{209}Bi targets. The energy loss in the Au foil reduced the beam energy to 31.6 MeV. Because of the degrader foils between the targets and the energy loss in the targets themselves, each Bi target was irra-

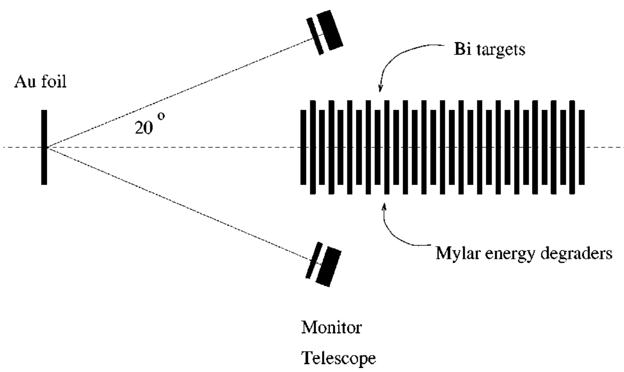

FIG. 1. Schematic representation of the on-line irradiation system.

diated at a lower incident ^{6}He energy. The range of incident energies seen by the Bi targets in the target stack spanned 31.6–20.0 MeV in the laboratory. The Bi targets were backed with 0.825 mg/cm^2 Mylar, had a nominal thickness of 1 mg/cm^2, and the removable Mylar energy degraders had a thickness of 0.825 mg/cm^2. The exact target thicknesses were measured individually by Rutherford backscattering techniques at Hope College after the experiment. During one of the activation runs a small number of the degraders were removed so that more of the targets would have a significant off-line count rate. The beam intensity, spatial distribution, and energy profile was determined with a position-sensitive ΔE-E telescope temporarily placed at the target location. In addition, elastic scattering from the thin Au target was used to monitor the beam intensity (and thus irradiation time profile) on-line. A schematic diagram of the targets, degraders, and monitor detectors is shown in Fig. 1.

The off-line counting system consisted of 32 Si surface barrier detectors, each 150 μm thick and 3 cm square. Each of the 16 irradiated Bi targets was placed between two closely spaced detectors so that the total solid angle subtended by the detectors for each target was $\approx$60% of 4π. The count rates were always low enough, $<$1 Hz, that system dead time could be ignored.

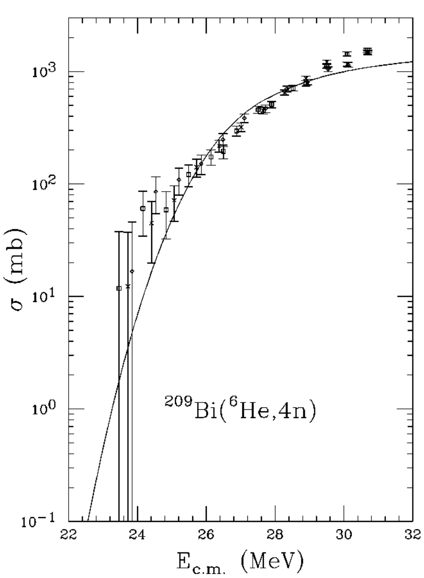

FIG. 2. Excitation function for four-neutron emission following the fusuion of ^{6}He+^{209}Bi. The three symbols correspond to the results from three separate irradiations and off-line measurements. The solid line is the prediction of the statistical model code PACE.

The targets were irradiated for approximately 17 h and then quickly transferred to the off-line counting system. The irradiated targets were then counted for approximately 20 h. Before irradiation, each of the targets was also counted for 24 h to establish the background α-activity levels.

Several factors are required to deduce the four-neutron evaporation cross sections from the integrated off-line α spectra. First, a normalized number of background counts were subtracted from the integrated counts. The integrated counts were also corrected for the solid angle, finite counting time, and the time to transfer the targets from the on-line scattering chamber to the off-line counting system (about 45 min). The corrected integrated count values correspond to the number of radioactive ^{211}At atoms present in each individual target at the end of the activation period.

Second, the number of ^{211}At atoms present at the end of the irradiation, from off-line counting, gives the four-neutron cross section after correcting for the decay of some of the ^{211}At during the irradiation. For this, the time structure of the beam intensity, as measured by the count rate of elastically scattered ^{6}He in the monitor detectors, was used.

Finally, in order to determine the absolute normalizaton, the actual ratio between the ^{6}He rate in the monitors and the primary beam current was directly measured with a detector temporarily positioned at the location of the center of the target stack. With this ratio and the total number of ^{6}He scattered into the monitors, the total number of incident beam particles was calculated and the absolute normalization of the cross section was determined. This ratio was monitored during the run by comparing the scattered ^{6}He in the monitors to primary beam current. Thus, the off-line data and on-line results were combined to determine the four-neutron cross section.

The measured cross section values need to be adjusted for the energy spread of the the beam. This spread is due to the acceptance of the *TwinSol* magnet and the possibility of populating excited states during the production of the secondary beam. The measured excitation function was deconvoluted using the measured energy distribution of the beam. The secondary ^{6}He beam energy profile (measured with a ΔE-E detector temporarily placed at the target location) was approximately Gaussian in shape with a full width at half maximum of 1.6 MeV.

The excitation function for the four-neutron evaporation channel is shown in Fig. 2 for center-of-mass energies from 23.5 to 30.7 MeV. The error bars shown are the statistical errors, dominated by the statistics of the number of α particles detected off-line and the off-line background count rates. There are small contributions to the statistical errors from solid angle simulations, monitor count rates, irradiation calculations, and the target thickness. The specific individual target thicknesses and measured average degrader thickness were used for all cross section determinations and energy-loss calculations. There are also systematic errors associated with the measurement. The systematic errors are estimated to be $\pm$350 keV in energy and 10% in cross section. The systematic uncertainty in the energy is based on variations in the measured energies in the monitors and measurements with detectors in the direct secondary beam. The systematic uncertainty in the cross section is mainly the result of systematic uncertainties in the target thickness and in the ratio of ^{6}He to primary beam current.

III. RESULTS AND DISCUSSION

The three symbols shown in Fig. 2 correspond to three independent measurements (separate irradiations) made of the excitation function. (The energies of the points are different in each case due to variations in individual target thicknesses and the particular degrader configuration.) The three separate results are shown, rather than averaging the measurements together, in order to give the reader a sense of the internal consistency of the data.

The solid line shown in Fig. 2 is the result of statistical model calculations done with the computer code PACE [15]. The results of the calculation, done with default parameters and taking the total fusion cross section from systematics, reproduce the data well. The agreement is even good at the lower energies where phase-space constraints limit the four-neutron yield and PACE often has difficulties accurately calculating the weak channels. Only the results at the highest energies are somewhat underpredicted by the model.

Above the barrier ($\approx$20.5 MeV) the measured four-neutron evaporation cross section does not show any features which could be conclusively attributed to the neutron-skin nature of the ^{6}He nucleus. On the other hand, the expected effects should be strongest at the Coulomb barrier where the extended neutron radius will provide the means of interaction. The four-neutron channel is limited by phase space to energies above the barrier. However, this result is quite important as it validates the behavior of the system and the model calculations at energies above the barrier. This is crucially important for the proper interpretation of future measurements nearer the barrier where the expected effects will be stronger.

IV. CONCLUSIONS

In conclusion, we present an improved measurement of the four-neutron evaporation cross section following fusion initiated with a radioactive nuclear beam. For energies somewhat above the Coulomb barrier to energies near the peak of the four-neutron evaporation yield, the agreement between the experimental measurements and the predictions of the statistical model are very good. No effects due to the neutron skin of ^{6}He are observed. However, this measurement establishes an important basis for understanding and interpreting future measurements involving this neutron-skin nucleus.

ACKNOWLEDGMENTS

This work was supported by the National Science Foundation under Grants No. PHY98-70262 (Hope College) and PHY94-02761 (Notre Dame). The *TwinSol* project was also funded by the National Science Foundation (PHY95-12199). V.G. was supported by the FAPESP (Brazil) while on leave from the Universidade Paulista.

[1] K. Ieki *et al.*, Phys. Rev. Lett. **70**, 730 (1993).
[2] Since the removal of either valance neutron or the core causes the system to be particle unstable, this system is termed a Borromean nucleus after the heraldic emblem of the medieval princes of Borromeo. The emblem is three interlocking rings arranged so that the removal of any one ring also uncouples the remaining two.
[3] C. Dasso, J. L. Guisardo, S. M. Lenzi, and A. Vitturi, Nucl. Phys. **A597**, 473 (1996).
[4] N. Takigawa, M. Kuratani, and H. Sagawa, Phys. Rev. C **47**, R2470 (1993).
[5] M. S. Hussein, M. P. Pato, L. F. Canto, and R. Donangelo, Phys. Rev. C **46**, 377 (1992); **47**, 2398 (1993).
[6] M. S. Hussein, Nucl. Phys. **A588**, 85c (1995).
[7] C. Dasso and A. Vitturi, Phys. Rev. C **50**, R12 (1994).
[8] I. Tanihata, D. Hirata, T. Kobayashi, S. Shimoura, K. Sugimoto, and H. Toki, Phys. Lett. B **289**, 261 (1992).
[9] J. J. Kolata, A. Morsad, X. J. Kong, R. E. Warner, F. D. Becchetti, W. Z. Liu, D. A. Roberts, and J. W. Jänecke, Nucl. Instrum. Methods Phys. Res. B **40/41**, 503 (1989).
[10] F. D. Becchetti and J. J. Kolata, in *Fourteenth International Conference on the Application of Accelerators in Research and Industry*, Denton, Texas, 1996, edited by J. L. Duggan and I. L. Morgan, AIP Conf. Proc. No. 392 (AIP, New York, 1997), p. 369–375.
[11] M. Y. Lee *et al.*, Nucl. Instrum. Methods Phys. Res. B **40/41**, 397 (1989).
[12] Yu. E. Penionzhkevich, Nucl. Phys. **A588**, 259c (1995).
[13] A. S. Fomichev, I. David, Z. Dlouhy, S. M. Lukyanov, Yu. Ts. Oganessian, Yu. E. Penionzkevich, V. P. Perelygin, N. K. Skobelev, O. B. Tarasov, and R. Wolski, Z. Phys. A **351**, 129 (1995).
[14] J. J. Kolata *et al.*, Phys. Rev. C **57**, R6 (1997).
[15] A. Gavron, Phys. Rev. C **21**, 230 (1980).